Water-Soluble Nanoparticles

DOI: 10.1002/anie.201407758

Highly Stable Water-Soluble Platinum Nanoparticles Stabilized by Hydrophilic N-Heterocyclic Carbenes**

Edwin A. Baquero, Simon Tricard, Juan Carlos Flores, Ernesto de Jesús,* and Bruno Chaudret**

Abstract: *Controlling the synthesis of stable metal nanoparticles in water is a current challenge in nanochemistry. The strategy presented herein uses sulfonated N-heterocyclic carbene (NHC) ligands to stabilize platinum nanoparticles (PtNPs) in water, under air, for an indefinite time period. The particles were prepared by thermal decomposition of a preformed molecular Pt complex containing the NHC ligand and were then purified by dialysis and characterized by TEM, high-resolution TEM, and spectroscopic techniques. Solid-state NMR studies showed coordination of the carbene ligands to the nanoparticle surface and allowed the determination of a ^{13}C–^{195}Pt coupling constant for the first time in a nanosystem (940 Hz). Additionally, in one case a novel structure was formed in which platinum(II) NHC complexes form a second coordination sphere around the nanoparticle.*

Although the synthesis and applications of metal nanoparticles (MNPs) have been widely studied, their surface chemistry after modification with organic ligands remains relatively unexplored.[1] The agglomeration of MNPs can be avoided by coordinating ligands to their surface.[2] N-heterocyclic carbenes (NHCs) have been shown to form fairly robust transition-metal complexes, which are excellent candidates for a large number of homogenous catalytic processes.[3] Surprisingly, the stabilization of MNPs with NHC ligands and, more specifically, the interaction between the metal surface and the NHC ligand, have rarely been studied.[4–13] Some of us have characterized the coordination of such ligands to ruthenium nanoparticles by solid-state NMR spectroscopy.[4] Furthermore, Pleixats and co-workers[6] and Glorius et al.[7,8] have reported the coordination NHCs to Pd nanoparticles, which were subsequently employed as catalysts. Additionally, NHCs have been used to synthesize Au[9,10] and Ag[11] MNPs as model systems for the formation of either conglomerates or 3D networks. We recently described the behavior of RuNPs as catalysts for the hydrogenation of arenes[5] and the synthesis of PtNPs as chemoselective catalysts for the hydrogenation of aromatic nitro compounds,[12] both stabilized by bulky NHCs. Although all of these studies involved organic solvents, the alternative use of water is very attractive for a wide range of applications of MNPs. After reporting the synthesis of Pt complexes with sulfonated NHC ligands in which the NHC–Pt bond was shown to be hydrolytically stable,[14,15] we reasoned that the dimethyl complexes depicted in Scheme 1 could potentially be suitable precursors for the synthesis of NHC-PtNPs by thermally activated ethane elimination.

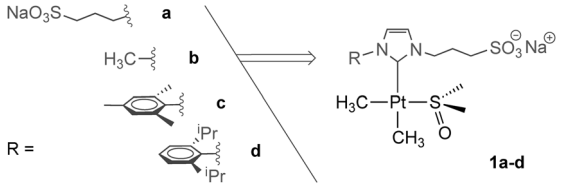

Scheme 1. Dimethyl (NHC)Pt^{II} complexes **1a–d**. R group on complexes **1a–d** given by the functional groups on the left.

Herein, and to our knowledge, we describe the first example of water-soluble MNPs supported by NHC ligands. The synthesized PtNPs were stable in water for months and could accommodate coordinated carbene ligands, as evidenced, for the first time, by the determination of a ^{13}C–^{195}Pt coupling between the ligand and the PtNP by NMR spectroscopy. As a test of the reactivity of these MNPs, we also studied the hydrogenation of styrene in water.

Aqueous solutions of complexes **1a–d** decompose at 80 °C to form the Pt nanoparticles **2a–d**, which gave a black, ink-like appearance to the solutions (Scheme 2). The PtNPs were purified by dialysis using a regular cellulose membrane. Although the colloidal solutions became neutral after work-up, the pH value measured before dialysis was higher than 9,

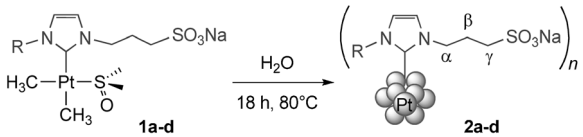

Scheme 2. Synthesis of PtNPs **2a–d** from Pt^{II} complexes **1a–d**.

[*] E. A. Baquero, Dr. J. C. Flores, Prof. Dr. E. de Jesús
Departamento de Química Orgánica y Química Inorgánica
Universidad de Alcalá, Campus Universitario
28871 Alcalá de Henares, Madrid (Spain)
E-mail: juanc.flores@uah.es
ernesto.dejesus@uah.es
Dr. S. Tricard, Prof. Dr. B. Chaudret
LPCNO; Laboratoire de Physique et Chimie de Nano-Objets
135, Avenue de Rangueil, 31077 Toulouse (France)
E-mail: chaudret@insa-toulouse.fr

[**] This work was supported by the Spanish Ministerio de Economía y Competitividad (project CTQ2011-24096) and CNRS and ANR (Siderus project ANR-08-BLAN-0010-03). We thank Y. Coppel (LCC) and P. F. Fazzini (LPCNO) for NMR and TEM/HR-TEM measurements, respectively. E.A.B. is grateful to the Universidad de Alcalá for a FPI Doctoral Fellowship and S.T. to the European Commission for a postdoctoral grant (PCIG11-GA-2012-317692).

Supporting information for this article is available on the WWW under http://dx.doi.org/10.1002/anie.201407758.

 © 2014 Wiley-VCH Verlag GmbH & Co. KGaA, Weinheim

as would be expected because of hydrolysis of some of the carbene ligands released during MNP formation. The colloidal suspensions of **2a–d** in water were homogeneous and highly stable in air, remaining totally dispersed without agglomeration or Pt^0 precipitation for at least six months. The PtNPs were obtained in notable yields (57–82% based on metal content determined by inductively coupled plasma mass spectrometry (ICP-MS) after purification).

Transmission electron microscopy (TEM) showed the formation of non-agglomerated, spherical nanoparticles with a fairly uniform size and diameters in the range 1.3–2.0 ± 0.4 nm depending on the ligand (Figure 1a and Figures S3–S5 in the Supporting Information). Use of the bulkiest ligands

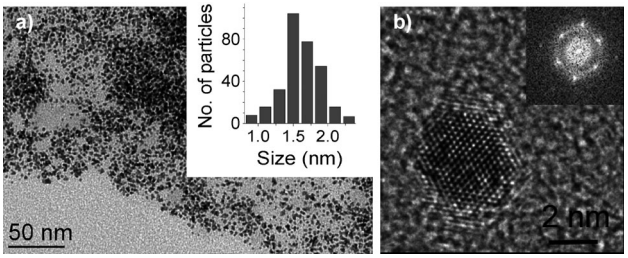

Figure 1. a) TEM image and size distribution, and b) HRTEM image with its corresponding FFT picture for PtNPs **2a**. Scale bar in (b) = 2 nm.

(c and d) provided the smallest PtNPs (1.3 ± 0.4 nm). High-resolution TEM (HRTEM) analyses unambiguously showed the highly crystalline character and face-centered cubic structure of PtNPs **2a–d**. Fast Fourier transformation (FFT) studies revealed reflections corresponding to the (111) and (002) atomic planes in all cases (Figure 1b and Figures S3–S5).

The PtNPs were characterized by attenuated total reflection Fourier transform infrared spectroscopy (ATR-FTIR) and ^{1}H NMR spectroscopy to confirm the presence of the NHC ligands (Figures S7–S10 and S13–S16). Only broad resonance signals were evident in the ^{1}H NMR spectra in D_2O of MNPs **2b–d**, whereas additional sharp signals were measured in the case of **2a** (see below). The ^{1}H resonance signals for the protons on the imidazole group and the propylsulfonate β- and γ-methylenes (labels assigned in Scheme 2) displayed chemical shifts comparable to the precursor **1** (δ = 7.4–7.1, 2.9 and 2.2 ppm, respectively), as did those for the methyl protons of the aryl groups in **2c** and **2d** (2.1–1.8 ppm for **2c**, and 1.3–0.9 ppm for **2d**). However, the signals corresponding to the α-methylene protons, the C*H* isopropyl (in **2d**), and the C*H* aryl (in **2c** and **2d**) were not detected. These protons are expected to be located close to the MNP surface and the absence of resonance signals is caused by the combined effect of an increased rigidity in the coordinated ligands after formation of the MNPs, slow tumbling of the particles which leads to rapid T_2 relaxation times, and the heterogeneity of the surface.[16] Similar effects have been observed in NHC-stabilized Au,[10] Pd,[8] or Ru nanoparticles.[4] Furthermore, the close proximity of the phenyl rings to the nanoparticle surface in **2c** and **2d** suggested by the ^{1}H NMR results reinforces the possibility of NHC-PtNP bonding by agnostic or π interactions, as we previously reported for NHC and 4-(3-phenylpropyl)pyridine ligands stabilizing RuNPs.[4,17] In contrast, the observation of resonance signals attributable to protons on the flexible propylsulfonate groups suggests that these chains point away from the particle, thus meaning that their ionic moieties are hydrated by the polar solvent. This interaction explains both the solubility and the high stability of PtNPs **2** in water.

We also investigated the coordination of the carbene ligands to the NPs by solid-state ^{1}H–^{13}C cross-polarization magic angle spinning (CP-MAS) NMR measurements (Figure 2). No resonance signals are detected attributable to protons on the Pt–CH_3 and Pt–DMSO moieties in the spectra of the PtNPs (Figure 2c for PtNP **2b**). These signals would be expected at circa δ = −5 and 40 ppm, respectively, considering the spectra of complexes **1a–d** (Figure 2 and Figures S17–S19). It appears that NHCs are the only ligands to remain attached to the nanoparticle surface (not counting water

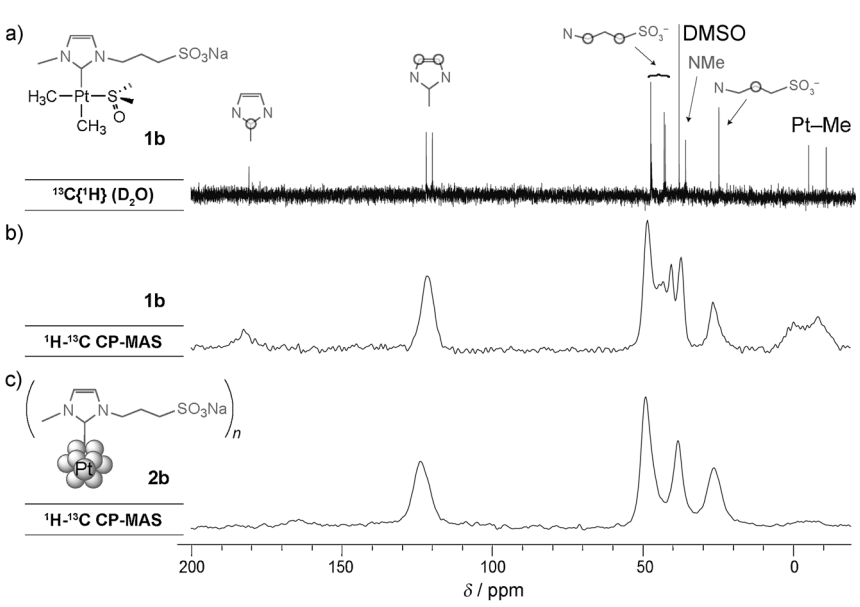

Figure 2. a) $^{13}C\{^1H\}$ NMR spectrum of complex **1b** in solution in D_2O and ^{1}H–^{13}C CP-MAS NMR spectra of b) **1b** and c) **2b** in the solid state.

molecules), thus resulting in broad ^{13}C signals in the expected regions for the imidazole methine carbon centers (δ = 124–122 ppm), the α, β, and γ-methylenes (δ = 49, 26, and 49 ppm), the methyl groups in **2c–d** (δ = 22–18 ppm), and the *C*H isopropyl carbon center in **2d** (δ = 28 ppm). Coordination of the NHC ligand through the carbenic carbon center is supported by the appearance of a resonance signal at

 © 2014 Wiley-VCH Verlag GmbH & Co. KGaA, Weinheim

approximately $\delta = 166$–172 ppm (not detected for **2c**) together with the absence of signal where signals for the carbonic carbon atoms of the imidazolium salts appeared ($\delta =$ 145–139 ppm). The signal for the carbenic carbon center is slightly shifted to higher field with respect to that found in **1** ($\delta = 185$–182 ppm) or in related [(NHC)Pt^0(dvtms)] complexes ($\delta = 200$–180 ppm; dvtms = divinyltetramethyldisiloxane).[14,18] We have previously observed the same effect in Pt/PVP/^{13}CO and Pt/dppb/^{13}CO nanoparticles (PVP = poly(*N*-vinyl-2-pyrrolidone); dppb = 1,4-bis(diphenylphosphino)butane) and proposed that it could be related to the Knight shift.[19]

The carbenic carbon resonance signal was very weak in the case of **2a**, **2b**, and **2d**, and undetectable for **2c**. To clear up uncertainties, we prepared nanoparticles **^{13}C-2c** containing a ^{13}C-labelled carbon in the C^2 position (i.e. the carbonic carbon atom) of the imidazolic ring (see Supporting Information for details). The size distribution of these labeled PtNPs was similar to that found for their nonlabeled analogues (1.3 ± 0.3 nm, Figure S6). The CP-MAS spectrum showed a clear resonance signal at the expected chemical shift of $\delta = 177$ ppm (Figure 3c and Figure S20). Moreover, the

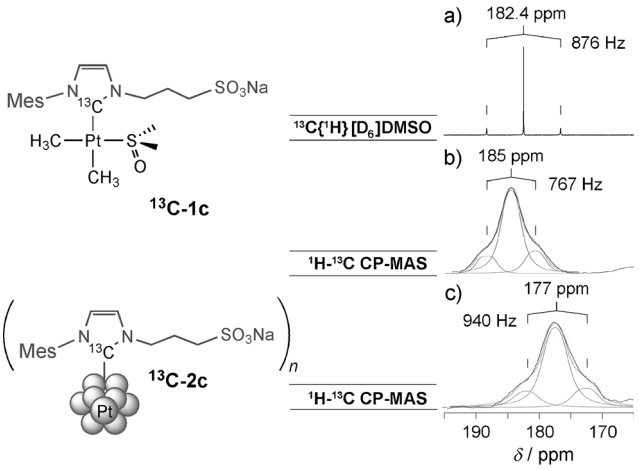

Figure 3. Resonance signals attributable to the Pt-bonded carbenic carbons in a) the ^{13}C{^{1}H} NMR spectrum of **^{13}C-1c**, and b), c) the ^{1}H–^{13}C CP-MAS NMR spectra of **^{13}C-1c** (b) and **^{13}C-2c** (c), displaying their corresponding deconvolution curves.

observation of a ^{13}C–^{195}Pt coupling involving a direct ligand–MNP interaction confirmed the attachment of the carbonic carbon center to the Pt surface. Line-shape deconvolution of the peak gave a coupling value equal to 940 ± 20 Hz. As expected, the carbene carbon atom is less strongly coupled to the ^{195}Pt center in **^{13}C-2c** than in molecular (NHC)Pt^0 complexes (around 1365 Hz),[18] although the interaction is still more intense than in the precursor **^{13}C-1c** (767 Hz), in which the oxidation state of the metal (+2) helps to decrease the magnitude of the coupling.[18,20] This coupling is an unambiguous indication of the carbene nature of the ligand coordinated to the Pt surface.

To determine the free sites on the surface, solid samples of **^{13}C-2c** were treated with ^{13}CO under mild conditions (room temperature, 1 bar). Unfortunately, the CP-MAS spectra of the resulting MNPs did not show any ^{13}CO coordination, although the IR spectra of samples recorded immediately after ^{13}CO treatment (within 5 minutes of removal of the gas) showed a band corresponding to CO adsorbed with a terminal mode of coordination (2010 cm^{-1}). However, this CO desorbed quite quickly and the band disappeared completely after 1 hour (Figure S12). The lability of CO as a ligand contrasts with the stability showed by the NHC coordination.

Even after 72 hours of dialysis, the ^{1}H NMR spectrum of nanoparticles **2a** showed the presence of sharp resonance signals in addition to the typical broad signals of the surface-coordinated NHC ligands (Figure S13). These sharp resonances are assigned to a bis(carbene) complex of formula $Na_3[PtMe(OH_2)(NHC)_2]$ (**3a**) based on the chemical shifts and integrals measured by ^{1}H NMR spectroscopy and the detection of the fragment $[\mathbf{3a}-Na-H_2O]^-$ in the ESI-MS spectrum of MNPs **2a** (Figure S23). Their persistence after dialysis is ascribed to the association, presumably by electrostatic interactions, of complex **3a** in a second coordination sphere around nanoparticle **2a** (nano-object **2a**/**3a**, Scheme 3). This interpretation is supported by diffusion-

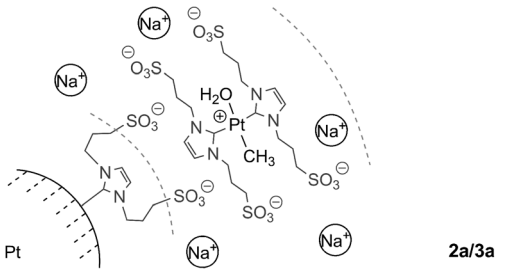

Scheme 3. Second coordination sphere in the nano-object **2a**/**3a**.

ordered NMR spectroscopy (DOSY), which gave almost the same diffusion coefficients for the nano-object components **2a** (broad signals, $2.5 \pm 0.3 \times 10^{-10}$ m^{2}s^{-1}) and **3a** (sharp signals, $2.8 \pm 0.3 \times 10^{-10}$ m^{2}s^{-1}), whereas those for the imidazolium salt (a, Scheme 1) and complex **1a** were higher (5.4 and $4.2 \pm 0.3 \times 10^{-10}$ m^{2}s^{-1}, respectively). DLS measurements consistently indicated a hydrodynamic diameter of 5.9 ± 1.8 nm for **2a** (i.e., the nano-object **2a**/**3a**) and of 2.2 ± 0.5, 1.6 ± 0.6, and 1.6 ± 0.7 nm for **2b**–**d**, respectively. These values are in good agreement with the sizes measured by TEM for **2b**–**d** (2.0 ± 0.3, 1.3 ± 0.4, and 1.3 ± 0.4 nm, respectively) but not for **2a** (1.6 ± 0.4 nm). As no saturation transfer was detected by 2D-NMR exchange spectroscopy (EXSY), complex **3a** does not exchange with the NHC ligands on the PtNP surface.

Further support for the formulation proposed for complex **3a** was obtained by treatment of the nano-object **2a**/**3a** with ^{13}CO at 3 bars in D_2O. Under these conditions, the complex *trans*-$Na_3[PtMe(^{13}CO)(NHC)_2]$ (**4a**) was formed (Scheme S1). The structure proposed for **4a** is supported by detection of the ion $[\mathbf{4a}-Na]^-$ in the ESI-MS spectrum of the resulting solution, the resonance signal in the ^{13}C NMR spectrum for the coordinated ^{13}CO ligand at $\delta = 175$ ppm, and

 © 2014 Wiley-VCH Verlag GmbH & Co. KGaA, Weinheim

a cross peak in the ^{1}H–^{13}C HMBC NMR spectrum between this ^{13}CO resonance signal and that of the protons on the Pt–CH_3 moiety (Figures S24–S27). Additionally, the ^{1}H–^{13}C coupling of 1.6 Hz between the signals attributable to the CH_3 and CO ligands is in agreement with a *trans* stereochemistry. Complex **4a** must remain attached to the MNP (nano-object **2a**/**4a**) as the DOSY measurements showed similar diffusion coefficients for this complex ($2.9 \pm 0.4 \times 10^{-10}$ $m^2 s^{-1}$) and the nano-object **2a**/**3a** ($2.8 \pm 0.3 \times 10^{-10}$ $m^2 s^{-1}$). A biscarbene complex (**3b**) was also detected by ^{1}H NMR spectroscopy during the formation of PtNPs from complex **1b** but not in the case of complexes with the more sterically demanding NHC ligands **1c** or **1d**. The $^{13}C(NHC)$–^{195}Pt coupling in complex **3b** (1042 Hz) is in accordance with reported values for bis(NHC) platinum(II) complexes (see the Supporting Information for other characterization data).[21] In contrast to **3a**, complex **3b** was washed away during dialysis, suggesting that the two flexible and anionic propylsulfonate groups are important for formation of the second coordination sphere in the nano-object **2a**/**3a**.

The PtNPs catalyzed the chemoselective hydrogenation of styrene to ethylbenzene at room temperature in water at 1 bar of H_2 (Table S1). The reactions were almost complete after 1 hour with Pt loadings of 0.4–0.6 mol%, except in the case of the nano-object **2a**/**3a**, where the second coordination sphere might hinder mass transfer to the reactive metal surface. The mono(NHC) Pt^{II} complexes **1** were much less active than their corresponding PtNPs even at higher catalyst loadings (Supporting Information). After extraction of the organic components with toluene, aqueous solutions containing MNPs **2d** were reused in nine consecutive recovery cycles with no noticeable modification of the catalytic performance (Figure S29) and with only a 0.44% loss of the starting Pt metal in the overall process (determined by ICP-MS analysis). TEM imaging showed that the MNPs retained their morphologies after the ninth recycling series (Figure S30).

In conclusion, unprecedented water-soluble PtNPs stabilized by NHC ligands can be obtained by thermal decomposition of dimethylplatinum(II) precursors containing sulfonated NHC ligands in water. Solution NMR spectroscopy studies, including diffusion measurements, revealed that the high stability and solubility of these MNPs in water is a consequence of the strong and inert coordination of the hydrophilic NHC ligand to the Pt surface. Unambiguous evidence for ligand coordination has been obtained by ^{13}C isotopic labeling of the carbenic carbon center, thus allowing observation of the first coupling (^{13}C–^{195}Pt) between ligands and PtNPs. Additionally, we have demonstrated the formation of a novel system involving the association of a nanoparticle with a molecular complex that remains coordinated to the particle but can still react with CO. This interesting finding may find a use in the design of associations between nanoparticles and molecular complexes with a view to, for example, cascade catalytic reactions. The results herein open up new routes towards catalytically active and water-stable metal nanoparticles.

Experimental Section

Synthesis of nanoparticles: The corresponding Pt complex **1** (0.945 mmol) was introduced into a 50 mL Schlenk flask and dissolved in deionized water (5 mL). The resulting colorless to pale-yellow solutions were stirred at 1000 rpm and heated at 80 °C for 18 hours. The resulting black solutions were left to reach room temperature slowly, filtered through a PTFE 0.2 μm filter, and dialyzed for 36 hours in water using a cellulose membrane (MWCO = 14000 Dalton).

Received: July 30, 2014
Revised: September 8, 2014
Published online: September 29, 2014

Keywords: N-heterocyclic carbenes · nanoparticles · platinum · solid-state NMR spectroscopy · surface characterization

[1] a) *Clusters and Colloids: From Theory to Applications* (Ed.: G. Schmid), Wiley-VCH, Weinheim, **1994**; b) *Nanoparticles. From Theory to Application* (Ed.: G. Schmid), Wiley-VCH, Weinheim, **2004**; c) A. Roucoux, K. Philippot in *Handbook of Homogeneous Hydrogenations* (Eds.: J. G. de Vries, C. J. Elsevier), Wiley-VCH, Weinheim, **2008**, pp. 217–256; d) *Nanoparticles and Catalysis* (Ed.: D. Astruc), Wiley-Interscience, New York, **2008**.

[2] L. S. Ott, R. G. Finke, *Coord. Chem. Rev.* **2007**, *251*, 1075–1100.

[3] a) *N-Heterocyclic Carbenes: From Laboratory Curiosities to Efficient Synthetic Tools* (Ed.: S. Diez-Gonzalez), The Royal Society of Chemistry, Cambridge, UK, **2011**; b) M. C. Jahnke, F. E. Hahn, *Top. Organomet. Chem.* **2010**, *30*, 95–129; c) F. E. Hahn, M. C. Jahnke, *Angew. Chem. Int. Ed.* **2008**, *47*, 3122–3172; *Angew. Chem.* **2008**, *120*, 3166–3216; d) O. Kühl, *Chem. Soc. Rev.* **2007**, *36*, 592–607.

[4] P. Lara, O. Rivada-Wheelaghan, S. Conejero, R. Poteau, K. Philippot, B. Chaudret, *Angew. Chem. Int. Ed.* **2011**, *50*, 12080–12084; *Angew. Chem.* **2011**, *123*, 12286–12290.

[5] D. Gonzalez-Galvez, P. Lara, O. Rivada-Wheelaghan, S. Conejero, B. Chaudret, K. Philippot, P. W. N. M. van Leeuwen, *Catal. Sci. Technol.* **2013**, *3*, 99–105.

[6] M. Planellas, R. Pleixats, A. Shafir, *Adv. Synth. Catal.* **2012**, *354*, 651–662.

[7] K. V. S. Ranganath, J. Kloesges, A. H. Schäfer, F. Glorius, *Angew. Chem. Int. Ed.* **2010**, *49*, 7786–7789; *Angew. Chem.* **2010**, *122*, 7952–7956.

[8] C. Richter, K. Schaepe, F. Glorius, B. J. Ravoo, *Chem. Commun.* **2014**, *50*, 3204–3207.

[9] E. C. Hurst, K. Wilson, I. J. S. Fairlamb, V. Chechik, *New J. Chem.* **2009**, *33*, 1837–1840.

[10] J. Vignolle, T. D. Tilley, *Chem. Commun.* **2009**, 7230–7232.

[11] X. Ling, N. Schaeffer, S. Roland, M.-P. Pileni, *Langmuir* **2013**, *29*, 12647–12656.

[12] P. Lara, A. Suárez, V. Collière, K. Philippot, B. Chaudret, *ChemCatChem* **2014**, *6*, 87–90.

[13] For the coating of planar metal surfaces with NHCs, see: a) T. Weidner, J. E. Baio, A. Mundstock, C. Große, S. Karthäuser, C. Bruhn, U. Siemeling, *Aust. J. Chem.* **2011**, *64*, 1177–1179; b) A. V. Zhukhovitskiy, M. G. Mavros, T. Van Voorhis, J. A. Johnson, *J. Am. Chem. Soc.* **2013**, *135*, 7418–7421; c) C. M. Crudden, J. H. Horton, I. I. Ebralidze, O. V. Zenkina, A. B. McLean, B. Drevniok, Z. She, H.-B. Kraatz, N. J. Mosey, T. Seki, E. C. Keske, J. D. Leake, A. Rousina-Webb, G. Wu, *Nat. Chem.* **2014**, *6*, 409–414.

[14] a) G. F. Silbestri, J. C. Flores, E. de Jesús, *Organometallics* **2012**, *31*, 3355–3360; b) E. A. Baquero, J. C. Flores, J. Perles, P.

 © 2014 Wiley-VCH Verlag GmbH & Co. KGaA, Weinheim

Gómez-Sal, E. de Jesús, *Organometallics* **2014**, DOI: 10.1021/om500753v.
[15] E. A. Baquero, G. F. Silbestri, P. Gómez-Sal, J. C. Flores, E. de Jesús, *Organometallics* **2013**, *32*, 2814 – 2826.
[16] a) E. Ramirez, L. Eradès, K. Philippot, P. Lecante, B. Chaudret, *Adv. Funct. Mater.* **2007**, *17*, 2219 – 2228; b) E. Ramirez, S. Jansat, K. Philippot, P. Lecante, M. Gomez, A. M. Masdeu-Bultó, B. Chaudret, *J. Organomet. Chem.* **2004**, *689*, 4601 – 4610.
[17] I. Favier, S. Massou, E. Teuma, K. Philippot, B. Chaudret, M. Gomez, *Chem. Commun.* **2008**, 3296 – 3298.
[18] G. Berthon-Gelloz, O. Buisine, J.-F. Brière, G. Michaud, S. Stérin, G. Mignani, B. Tinant, J.-P. Declercq, D. Chapon, I. E. Markó, *J. Organomet. Chem.* **2005**, *690*, 6156 – 6168.
[19] S. Kinayyigit, P. Lara, P. Lecante, K. Philippot, B. Chaudret, *Nanoscale* **2014**, *6*, 539 – 546.
[20] a) D. Tapu, D. A. Dixon, C. Roe, *Chem. Rev.* **2009**, *109*, 3385 – 3407; b) B. M. Still, P. G. A. Kumar, J. R. Aldrich-Wright, W. S. Price, *Chem. Soc. Rev.* **2007**, *36*, 665 – 686; c) K. A. Netland, A. Krivokapic, M. Tilset, *J. Coord. Chem.* **2010**, *63*, 2909 – 2927.
[21] a) O. Rivada-Wheelaghan, B. Donnadieu, C. Maya, S. Conejero, *Chem. Eur. J.* **2010**, *16*, 10323 – 10326; b) O. Rivada-Wheelaghan, M. A. Ortuño, J. Díez, A. Lledós, S. Conejero, *Angew. Chem. Int. Ed.* **2012**, *51*, 3936 – 3939; *Angew. Chem.* **2012**, *124*, 4002 – 4005; c) O. Rivada-Wheelaghan, M. Roselló-Merino, M. A. Ortuño, P. Vidossich, E. Gutiérrez-Puebla, A. Lledós, S. Conejero, *Inorg. Chem.* **2014**, *53*, 4257 – 4268.

 © 2014 Wiley-VCH Verlag GmbH & Co. KGaA, Weinheim